

## DESIGN OF X-RAY TARGETS FOR HIGH ENERGY LINEAR ACCELERATORS IN RADIOTHERAPY\*

By E. B. PODGORŠAK, Ph.D., J. A. RAWLINSON, M.Sc.,  
M. I. GLAVINOVIĆ, B.Sc., and H. E. JOHNS, Ph.D.  
TORONTO, ONTARIO, CANADA

IN a recent paper Rawlinson and Johns<sup>6</sup> showed that a 25 MeV linear accelerator (Varian Clinac-35) produced an inferior beam of photons to a 25 MeV betatron (Allis Chalmers). In fact, from a depth dose point of view, the linac's beam was equivalent to the beam produced by the betatron when it was operated at 16 MeV. The reasons for this were attributed to differences in the design of the target and the flattening filter in the 2 machines. The betatron employs a thin tungsten target and an aluminum flattening filter, while the linac uses a thick tungsten target and a tungsten flattening filter.

The purpose of this paper is to present the experimental results of our further investigation of this problem and to suggest some methods for improving the x-ray beams from linacs used in radiotherapy. In the present experiments the 25 MeV electron beam from the linear accelerator was used to produce x-rays in targets of different atomic numbers. The x-ray beams were flattened with flattening filters made of various materials. Using these targets and filters, depth doses and x-ray yields were measured both along the central axis of the beam and at different angles to the central axis.

We have found that by using a *thick aluminum* target and an *aluminum flattening filter* in the linear accelerator we can obtain the same depth dose distribution as from the Allis Chalmers betatron operating at the same energy. Furthermore, the x-ray yield in the forward direction is the same within a few per cent, whether we use a thick aluminum or thick lead target. It thus appears that thick targets in linear accelerators should be made of low atomic

number materials. For such targets a more penetrating beam is produced and the yield in the forward direction is as good as from a high atomic number material.

### EXPERIMENTAL APPARATUS AND PROCEDURES

Experiments reported in this paper have been carried out at the Ontario Cancer Institute in Toronto using the electron beam from a Varian Clinac-35 linear accelerator. The schematic diagram of the experimental apparatus is shown in Figure 1. As normally used in radiotherapy, the electron beam is bent first through 57°, next focused by 2 quadrupole lenses, and then bent 90° to hit a tungsten target where it produces an x-ray beam which emerges at port No. 3. This port was not used in our experiments because of the difficulties in removing the linac head (collimators, transmission ion chamber, etc.) to obtain an unobstructed electron beam. Instead, in our studies we turned off the 90° bending magnet allowing the electron beam to emerge at port No. 2 through a thin beryllium window. The extracted electron beam was then made to produce x-rays in our own targets which were secured to the linac in the position shown in the diagram. With the 90° bending magnet turned off, the electron beam was focused onto the target into a circle of ~3 mm diameter. The experimental apparatus will be discussed in more detail in the following sections.

### TARGETS

The targets were cylinders of 5 cm diameter positioned in air 3 cm from the beryllium exit window. Their thicknesses

\* From the Physics Division, Ontario Cancer Institute, Toronto, Ontario, Canada.

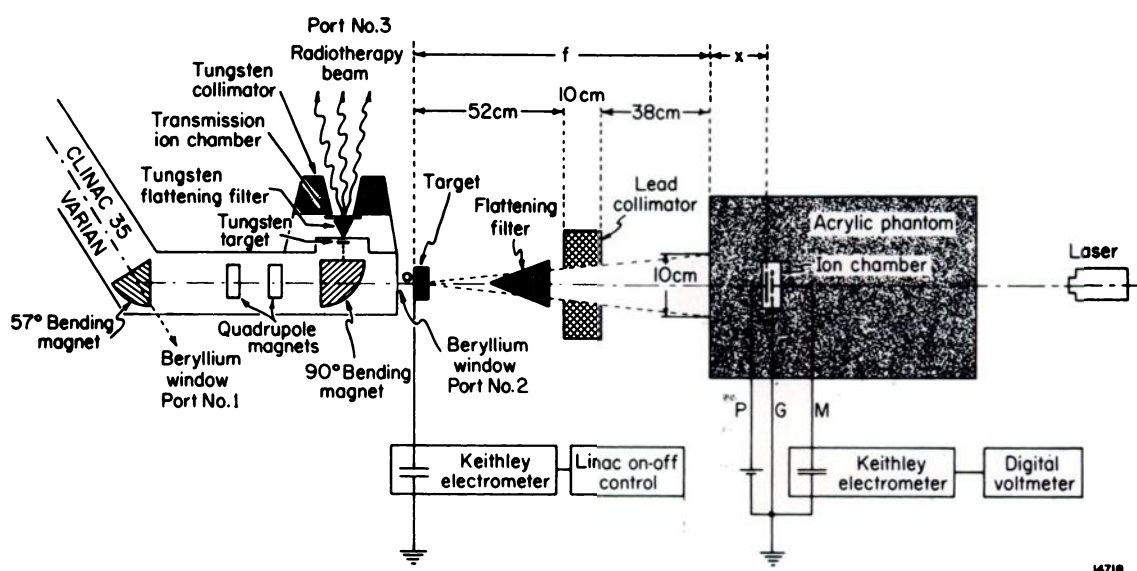


FIG. 1. Schematic diagram of the complete experimental apparatus.

were chosen to be equal to the mean range of 25 MeV electrons in the target material. This ensured a complete stopping of the incident electrons with minimum attenuation of the x-ray beam produced in the target. Using range values tabulated by Berger and Seltzer<sup>1</sup> the target thicknesses were 0.9 cm and 5.2 cm for lead and aluminum, respectively.

#### FLATTENING FILTERS

The flattening filters were made of lead and aluminum. They were conically shaped with a base diameter of 12 cm and a height of 3.4 cm and 25 cm for the lead and aluminum filters, respectively. The filters produced a beam which was uniform to within  $\pm 10$  per cent over a field of diameter 40 cm at a phantom depth of 10 cm and a source to chamber distance of 100 cm. The filter was positioned on the beam axis and arranged to move along the axis on a V block (not shown in the Figure) thus enabling us to introduce more or less of the filter material into the x-ray beam. The beam flatness could be quickly checked using our matrix dosimeter<sup>4</sup> placed behind the flattening filter and the position of the filter then moved slightly to give the optimum beam.

#### COLLIMATORS

The collimator used for depth dose measurements along the central axis was made of lead with a tapered hole at the center designed to give a 10 cm diameter circular field at 100 cm from the target. For the depth dose measurements at an angle to the central axis, the collimator was designed to give a 3 cm diameter circular field at 125 cm from the target. For these latter measurements the trolley carrying the various components was rotated about point O shown in Figure 1.

#### PHANTOM

The phantom was made of acrylic slabs with a density of 1.18 g/cm<sup>3</sup> and an area 12×12 inches. Into one of these slabs a cavity was milled to house the special ion chamber. To change the depth in the phantom, slabs were placed in front of the chamber and the phantom moved away from the target so as to keep the source to surface distance (SSD) equal to 100 cm.

#### DETECTOR

A cylindrical polystyrene end window ion chamber was built with a sensitive volume of 2 cm diameter and 1.2 mm depth. The polarizing electrode, P, was made of

50 microns aluminized mylar and connected to a 400 volts power supply. A thin coat of aquadag covering a circle (2 cm diameter) on the bottom surface of the chamber served as the measuring electrode, M. The charge collected here due to radiation was measured by a Keithley amplifier whose output was fed into a digital voltmeter, as shown in Figure 1. The guard ring, G, which was electrically insulated from the measuring electrode, and grounded, was a 5 mm wide aquadag ring painted around the measuring electrode leaving a gap of about 0.5 mm. The chamber leakage current was less than  $10^{-12}$  A, while the charge collected on the measuring electrode after a typical exposure of 1 second was on the order of  $10^{-9}$  C which shows that the chamber leakage currents were not a serious problem. The collection efficiency of the chamber was measured to be better than 99 per cent under the conditions used in the experiments.

#### MONITOR

The linac was arranged so that it was turned off after a given exposure. To do this the target was electrically insulated from ground and the charge delivered to it during the exposure was measured by a Keithley electrometer, whose output voltage (0-3 volts) was compared with a preset voltage by an operational amplifier. The positive output of the amplifier was used to trigger a relay which turned the linac beam off, when the charge collected on the target reached the preset value. Exposures delivered this way were reproducible to better than 1 per cent. At 80 pulses per second, a pulse width of 1.8  $\mu$ sec and a pulse height of 40 mA, the charge collected on the target was about  $6 \times 10^{-6}$  C/sec.

#### ALIGNMENT OF THE COMPONENTS

The flattening filter, collimator and phantom were mounted on a trolley which could be placed in a fixed position with respect to the linac. One of the experimental problems that was encountered in our measurements was the alignment of

the apparatus. It is virtually impossible to obtain good beam flatness data without making sure, ahead of time, that the electron beam axis coincides with the axis of the apparatus; *i.e.*, with the central axes of the flattening filter, the collimator and phantom. The procedure was as follows: (1) 2 pieces of radiation sensitive paper,\* one 2 cm and the other 10 cm from the beryllium window, were exposed to the electron beam. The discolored spots produced by the radiation on the papers defined the electron beam axis. (2) A laser, located about 2 m from the window, was oriented so that its light beam was directed onto the beryllium window through the centers of the 2 spots on the radiation sensitive paper. In this way, the laser beam was made to coincide with the electron beam axis and further alignment procedure for the rest of the components was easy.

#### DEPTH DOSE MEASUREMENTS

Depth doses were measured in the acrylic phantom from the surface to a depth of  $\sim 25$  cm. After each exposure the charge collected on the ion chamber measuring electrode was determined. Readings were obtained with both positive and negative polarities on the chamber ( $\pm 400$  V) and the results averaged. Since published depth doses are generally obtained using water phantoms, a correction was made to transform our acrylic depth dose measurements into doses in water. The transformation involves both an electron density correction and an inverse square law correction. If  $x$  is the depth in the acrylic phantom as shown in Figure 1 and  $D_a(x)$  is the dose measured in acrylic at  $x$ , one obtains the dose in water  $D_w$  at a depth in water  $x' = \{\rho_a/\rho_w\}x$  using the following expression:

$$D_w(x') = D_a(x) \left\{ \frac{f+x}{f+x'} \right\}^2, \quad (1)$$

\* Available from Vickers Ltd., Radiation and Nuclear Engineering Division, South Merston Works, P.O.B. 8, Swindon, Wilts, U.K.

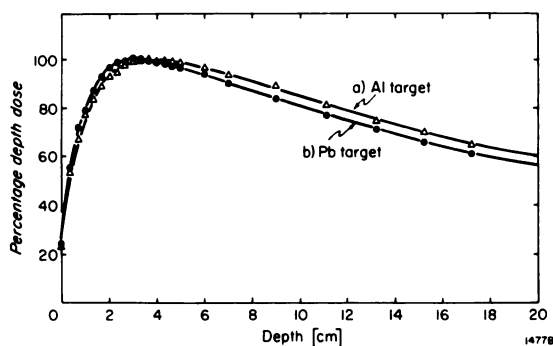


FIG. 2. Central axis percentage depth dose curves in water of unflattened x-ray beams produced by 25 MeV electrons impinging on (a) aluminum thick target, and (b) lead thick target. Circular field size with 10 cm diameter at a target to surface distance of 100 cm.

where  $f$  is the source to phantom surface distance and  $\{\rho_a/\rho_w\}$  is the ratio of the electron densities in acrylic and water. For these 2 materials this is also close to the ratio of actual densities.

## EXPERIMENTAL RESULTS

### THICK X-RAY TARGETS

In this section we discuss the differences in x-ray beams produced by various targets, using *no* flattening filter. Figure 2 shows depth dose curves obtained from aluminum and lead targets at a source to phantom distance of 100 cm and a field size of 10 cm diameter at the phantom surface. A comparison between the 2 curves in Figure 2 shows that the aluminum target gives a more penetrating beam than the lead target, its surface dose is slightly lower and the depth of the maximum dose is larger (4 cm *vs.* 3 cm). A measurement of the depth dose curve of x-rays produced by a copper target (not shown in Figure 2) revealed that it lay between the curves for lead and aluminum. While the curves of Figure 2 are of no practical value, because the x-ray beam is unflattened, they do show that the beam from the aluminum target is more penetrating than the beam produced in lead.

The central axis x-ray yield of different targets was measured as a function of the target atomic number  $Z$ . The results are

shown in Figure 3 where, for a given charge delivered to the target, the actual ion chamber current is plotted *versus* depth. It is evident that the aluminum target gives the highest yield, although the differences between the peak currents from aluminum, copper and lead targets are small. This result is surprising since one usually assumes that the yield increases with  $Z$ .

The findings summarized in Figures 2 and 3 suggest that low  $Z$  material should be used as the target in radiotherapy linacs. The beams so produced are more energetic than those from high  $Z$  targets and the useful x-ray outputs are just as high.

### FLATTENING FILTERS

All high energy x-ray machines used in radiotherapy employ flattening filters to produce a uniform depth dose distribution over the maximum field size used. In this section are presented the results of an investigation into the characteristics of the flattened x-ray beams as a function of the target and filter material.

Depth doses were measured for the flattened beams with a circular field size of 10 cm diameter at the target to surface distance of 100 cm using the experimental arrangement shown in Figure 1. We found, as predicted by Rawlinson and Johns,<sup>6</sup> that a high  $Z$  flattening filter material

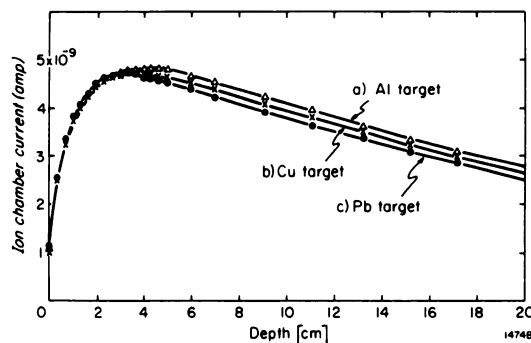


FIG. 3. Ion chamber current as a function of the depth in water for unflattened x-ray beams produced by 25 MeV electrons impinging on (a) aluminum thick target, (b) copper thick target, and (c) lead thick target. Field size 10 cm diameter at a target surface distance of 100 cm.

(lead in our experiments) softens a beam, while a low  $Z$  flattening filter material (aluminum in our experiments) hardens it. The most penetrating x-ray beam was obtained with an aluminum target/aluminum flattening filter combination, while a lead target/lead flattening filter combination rendered the least penetrating beam. The depth dose curves for these 2 extreme cases are shown in Figure 4. The lead target/lead flattening filter combination gives a depth dose curve which is almost identical to the one produced by the Clinac-35 beam which is used in radiotherapy. This is not unexpected since the Clinac-35 employs a tungsten target/tungsten flattening filter combination in the radiotherapy x-ray mode and the atomic numbers of tungsten and lead are similar.

In Figure 5, our experimental central axis depth dose curve obtained with the aluminum target/aluminum flattening filter combination is compared with the central axis depth dose curve from the Allis Chalmers 25 MeV betatron. The 2 curves are almost identical. This shows that from a depth dose point of view a considerable improvement of the linac x-ray beams is achieved with a thick, low  $Z$  target/low  $Z$  flattening filter combination as compared to the high  $Z$  target/high  $Z$  flattening filter combination generally used.

A summary of our central axis depth

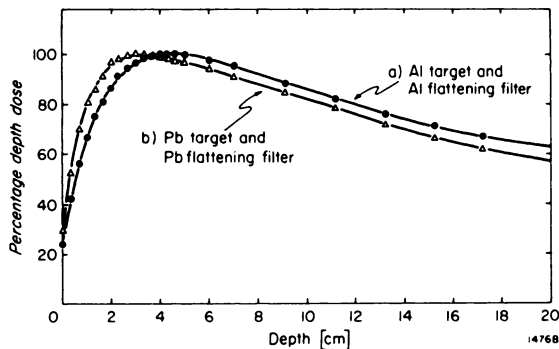


FIG. 4. Central axis depth dose curves of flattened x-ray beams in water produced by 25 MeV electrons impinging on a thick target: (a) aluminum target and aluminum flattening filter; and (b) lead target and lead flattening filter. Field size 10 cm diameter at a target to surface distance of 100 cm.

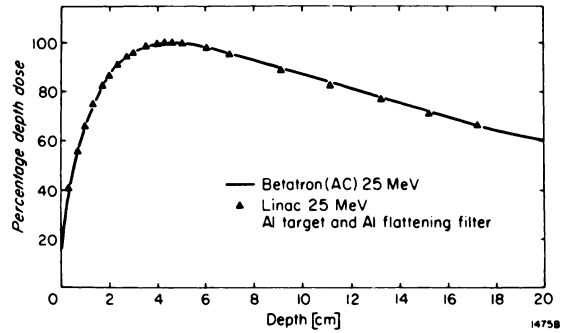


FIG. 5. Percentage depth dose curve from an Allis Chalmers 25 MeV betatron (solid line) compared to 25 MeV linac data obtained using an aluminum target and an aluminum flattening filter ( $\blacktriangle$ ).

dose measurements is given in Table I. The depth dose data measured for x-ray beams produced by lead and aluminum targets and flattened with lead and aluminum filters are shown in Columns 2, 3, 6 and 7. For comparison purposes we also show the depth dose data of the unflattened beams produced by the 2 targets (Columns 1 and 5, also shown in Figure 2), as well as the depth dose data for the Varian Clinac-35 and the Allis Chalmers 25 MeV betatron (Columns 4 and 8, respectively). Most of the conclusions that can be drawn from this Table were already mentioned, so that now only a brief summary will be given.

(1) Aluminum targets give a more penetrating beam than lead targets (compare Columns 1 and 5).

(2) Lead flattening filters soften the beam, although the effect is not very pronounced (compare Columns 1 with 3 and 5 with 6).

(3) Aluminum flattening filters harden the beam (compare Columns 1 with 2 and 5 with 7).

(4) The Varian Clinac-35 radiotherapy beam is almost identical to the beam produced by a lead target/lead flattening filter combination (compare Columns 3 and 4).

(5) The Allis Chalmers betatron beam is almost identical to the beam produced by an aluminum target/aluminum flattening filter combination (compare Columns 7 and 8).

TABLE I\*

Flattening Filter (cm) Depth in Water	Lead Target			Linac	Aluminum Target			Betatron
	None (1)	Al (2)	Pb (3)	Radio- therapy Beam (4)	None (5)	Pb (6)	Al (7)	Radio- therapy Beam (8)
0	24.3	26.4	30.4	—	23.5	26.7	23.4	—
0.1	33.0	29.5	36.0	20.5	32.0	32.5	27.0	18.8
0.25	50.5	35.5	45.0	38.5	42.5	41.5	35.5	30.0
0.50	62.5	49.8	56.1	59.0	60.3	56.0	46.0	45.3
0.75	74.5	58.1	72.3	72.4	71.2	67.3	57.5	55.5
1.0	80.7	66.8	78.7	80.1	77.2	76.5	66.5	64.9
1.5	89.5	79.0	89.2	90.3	85.9	86.1	78.3	77.3
2.0	95.7	87.8	95.7	95.5	91.1	91.6	86.1	86.0
2.5	98.7	94.3	98.9	98.7	95.3	95.3	92.5	91.9
3.0	99.8	97.7	100.0	99.9	97.8	97.8	96.1	95.6
3.5	100.0	99.3	99.8	100.0	99.2	99.4	98.0	98.1
4.0	99.2	100.0	99.3	99.7	100.0	100.0	99.1	99.5
4.5	97.8	99.4	98.6	99.0	99.7	99.2	99.8	100.0
5.0	96.7	98.4	97.3	97.6	98.7	98.0	100.0	99.8
6.0	93.7	96.1	93.8	94.5	96.4	95.4	98.2	98.2
7.0	90.6	93.3	90.8	91.4	93.6	92.4	95.5	95.9
8.0	87.3	90.7	87.9	88.4	90.6	89.2	92.4	92.9
9.0	84.1	87.8	84.7	85.2	87.4	85.9	89.6	90.2
10.0	81.2	84.8	81.4	81.9	84.0	82.7	86.8	87.4
11.0	78.1	81.8	78.5	78.8	80.8	79.7	83.7	84.6
12.0	75.2	78.8	75.5	75.9	77.7	76.7	80.8	81.6
13.0	72.2	76.0	72.6	72.9	74.7	73.4	77.7	78.5
14.0	69.4	73.2	69.6	70.1	71.9	70.5	74.8	75.4
15.0	66.6	70.3	66.7	67.2	68.9	67.7	72.1	72.5
16.0	64.1	67.7	64.2	64.5	66.3	65.0	68.8	69.6
17.0	61.6	65.5	61.8	61.8	63.9	62.4	66.7	66.7
18.0	59.2	63.5	59.6	59.2	61.6	60.0	64.6	64.3
19.0	56.8	61.5	57.2	56.7	59.2	57.8	62.1	62.1
20.0	54.5	59.5	54.8	54.5	57.0	55.7	59.9	60.0
21.0	52.4	57.4	52.6	52.5	55.0	53.6	57.6	57.7
22.0	50.1	55.4	50.6	50.3	52.8	51.1	55.7	55.9
23.0	47.8	53.5	48.3	48.2	50.7	49.7	53.6	53.7

\* Depth dose data obtained from an electron beam of 25 MeV using various combinations of filters and targets. The linac data are for a Varian machine with a tungsten target and filter, while the betatron data are for an Allis Chalmers machine using a thin tungsten target and aluminum filter. Field size 10 cm circle at 100 cm. When flattening filters were used, the field was flattened to  $\pm 10$  per cent over 90 per cent of the field.

## ANGULAR DISTRIBUTION OF X-RAYS

We have already shown experimentally that the central axis x-ray yield is essentially independent of the target atomic number  $Z$ . On the other hand, the theories of x-ray production<sup>2,3,5</sup> predict a yield that increases with  $Z$ . These 2 apparently contradictory statements can perhaps be reconciled, if one keeps in mind that the theories are concerned with the *total* yield integrated over all angles, while our mea-

surements so far presented are for the forward direction only. In order to gain a better understanding of this problem we have investigated the properties of the x-ray beam at various angles from the direction defined by the electron beam. For these measurements a small circular beam of 3 cm in diameter at a fixed target to surface distance of 125 cm was used. In addition, the diameter of the cylindrical target was increased to 10 cm. Depth dose

distributions were measured for both the aluminum and lead targets at various angles  $\theta$  up to  $60^\circ$  from the central axis. In Table II we show the relative maximum doses normalized to 100 per cent for the beam produced at  $0^\circ$  by the aluminum target and obtained from the depth dose data at various angles  $\theta$ . It is evident that as the angle  $\theta$  increases, the value of the dose decreases rapidly. Furthermore, at large angles much more radiation is emitted by the high  $Z$  material, and even at  $10^\circ$  almost twice as much radiation is emitted from lead as from aluminum.

Table II does not give a complete picture, since not only does the number of photons decrease with angle but also the photon spectrum changes. This can be seen from Figure 6 which shows percentage depth dose curves for angles  $\theta=0, 10, 20$  and  $30^\circ$  or from Table III, where we show the depths of the dose maxima in centimeters for various angles  $\theta$ . For both the aluminum and lead targets, the larger the angle the smaller is the depth of maximum dose, indicating a lower effective beam energy. Again, as in Figure 2, the central axis beam ( $\theta=0$ ) produced by the aluminum target is more penetrating than that produced by the lead target. At  $\theta\sim 10^\circ$ , however, both targets produce almost equally penetrating beams, and at angles larger than  $10^\circ$  the lead target gives a more penetrating beam than the aluminum target. It should be emphasized however that in radiotherapy one is interested in angles less than  $10^\circ$ , in which case the aluminum target produces a

more penetrating beam than the lead target.

We have used the depth dose data obtained at different angles to determine approximately the total energy emitted into a given solid angle. To do this the depth dose curves were extrapolated to infinity and the integral dose under each curve was calculated. The photon energy fluence per incident electron at a target to surface distance of 125 cm was then determined as a function of angle  $\theta$ . This is shown by the dashed curves in Figure 7. The absolute fluence values shown in the figure are of limited accuracy because of the many approximations used in the calculation. Nevertheless, one can draw some conclusions from the relative shapes of the 2 fluence curves shown in the figure. In the forward direction, the fluences for aluminum and lead are essentially the same, but as the angle is increased beyond  $5^\circ$  the fluence from aluminum falls much more rapidly than that from lead. This may be explained as follows: in a high  $Z$  material larger angular deviations of the electron are produced than in a low  $Z$  material. The deviated electrons then produce x-rays, so more radiation is emitted at large angles from a lead than from an aluminum target. Furthermore, the electrons in lead suffer fewer collisions in being deviated to a large angle  $\theta$  than those in aluminum, so they have greater energy and thus produce more energetic x-rays.

The total x-ray energy emitted by the targets can be calculated by integrating the fluence over the surface of a sphere of a radius equal to the source to phantom distance (125 cm). This integral is plotted in Figure 7 (solid line curves) as a function of angle  $\theta$  from  $\theta=0$  to  $\theta=90^\circ$ . It is evident that the photon yield in the forward half sphere of the lead target ( $\sim 20$  per cent) is more than a factor of 2 larger than that of the aluminum target ( $\sim 9$  per cent). Thus, the total x-ray yields do depend on the atomic number  $Z$  of the target: the higher the  $Z$  the larger the x-ray yield. Over the range of angles of interest in

TABLE II\*

Target	Angle $\theta$ (deg.)					
	0	5	10	20	30	45
Aluminum	100	44.5	16.8	6.5	2.4	0.7
Lead	95	54.6	31.7	15.1	7.5	3.7

\* Dose maxima as a function of angle for targets of aluminum and lead. The values are normalized to 100 per cent for aluminum at  $0^\circ$ .

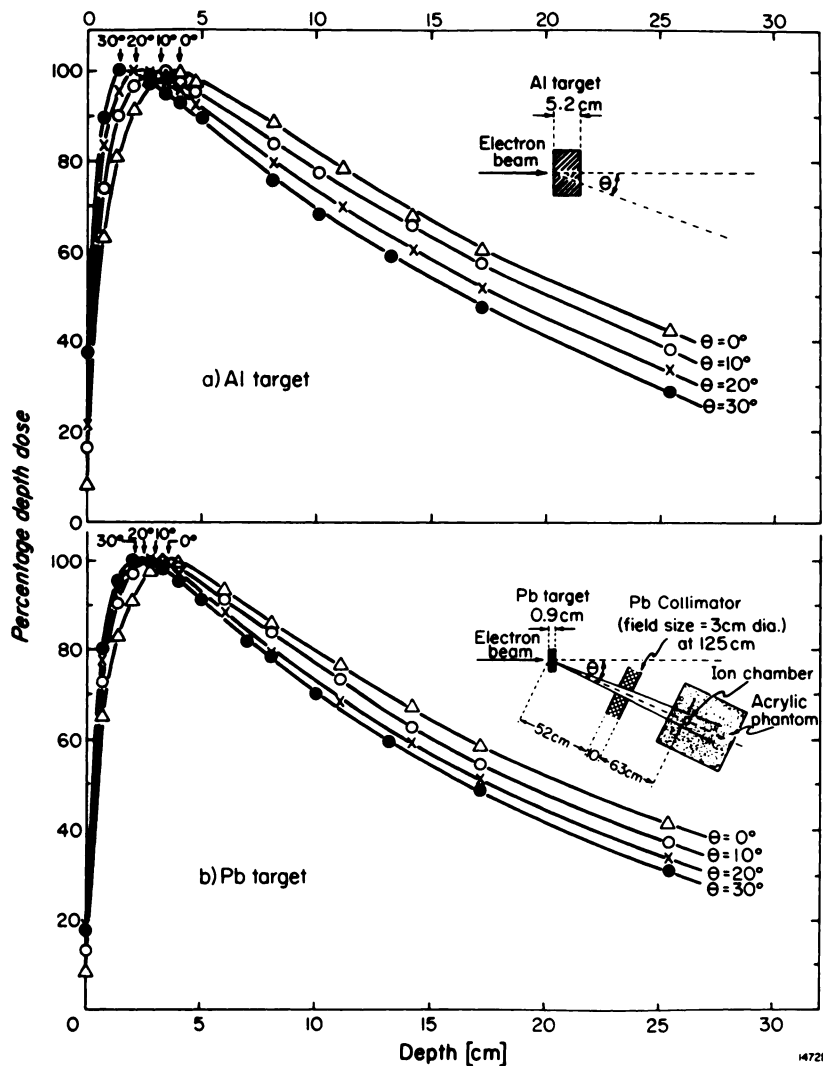


FIG. 6. Percentage depth dose curves of unflattened beams produced by (a) aluminum target and (b) lead target, for various angles from the central axis. Field size 3 cm diameter at a target to surface distance of 125 cm.

radiotherapy, however, the x-ray yields of aluminum and lead are not much different.

#### FIELD FLATNESS

We have shown in previous sections that an aluminum target produces a more energetic x-ray beam than a lead target, indicating that aluminum targets should be used in radiotherapy linear accelerators. But we have also shown that the x-rays from the aluminum target are more forward peaked than those from a lead target,

TABLE III\*

Target	Angle $\theta$ (deg.)					
	0	5	10	20	30	45
Aluminum	4.1	3.8	3.1	2.2	1.7	1.3
Lead	3.5	3.4	3.0	2.6	2.3	2.0

\* Depths of dose maxima (in cm) as a function of angle for targets of aluminum and lead.

which suggests that in practice it might be difficult to flatten the beam produced by an aluminum target over an extended field. That this is not the case can be seen from Figure 8, which shows the results of our field flatness measurements obtained by scanning a Baldwin-Farmer ion chamber across the beam at a target to detector distance of 100 cm and a depth in the acrylic phantom of 10 cm. The dashed curves of Figure 8 show the unflattened and flattened profiles produced by the lead target, while the solid curves show the corresponding profiles produced by the aluminum target. In both cases, the filters have been designed to flatten the beam over a circular field size of at least 40 cm diameter. As can be seen from the figure, in order to flatten a beam of a given field size, the unflattened beam from the aluminum target has to be attenuated more than the one from the lead target. However, this difference is small and results in an effective output from the flattened aluminum beam which is only 20 per cent less than that from the flattened lead beam.

The variation of beam flatness with depth in the phantom was studied by comparing flatness measurements obtained at various

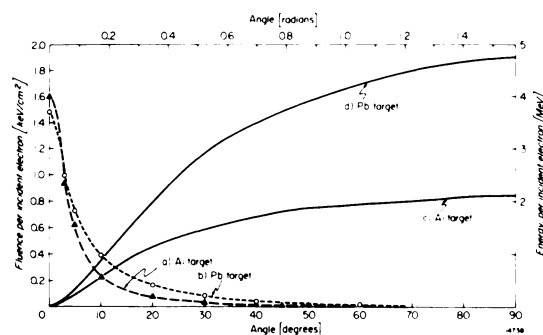


FIG. 7. The dashed curves represent the energy fluence ( $dE/dA$ ), per incident 25 MeV electron as a function of the angle  $\theta$  from the central axis (a) for an aluminum target and (b) for a lead target. The solid curves represent the integral of the fluence,  $\int_0^{2\pi} \int_0^\theta (dE/dA) R^2 \sin \theta d\theta d\phi$ , over the surface of a sphere with radius,  $R$ , equal to the target to phantom surface distance (125 cm). This integral is equal to the x-ray energy emitted into a solid angle,  $\Omega$ , defined by the angle  $\theta$ .

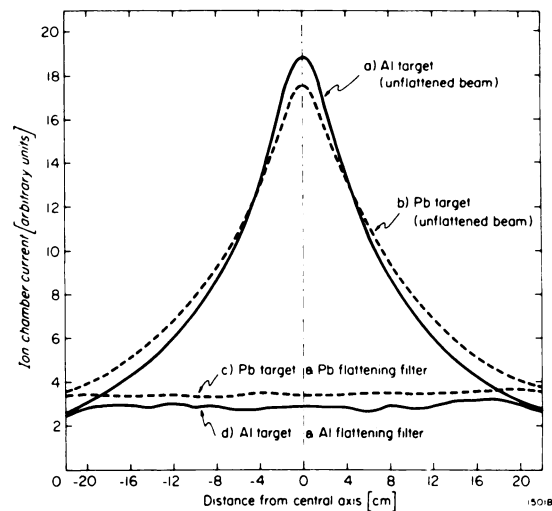


FIG. 8. A comparison between unflattened and flattened x-ray beams produced by 25 MeV electrons impinging on an aluminum target (solid line curves) and on a lead target (dashed curves).

depths (3 cm, 10 cm, 20 cm). One would anticipate a larger variation of flatness with depth in the case of the aluminum target/aluminum filter combination as compared to the lead target/lead filter combination. Although this was found to be true, the measured variation in both cases was small. For aluminum, assuming a perfect beam flatness at 10 cm depth, the uniformity across the beam at depths of 3 cm and 20 cm would be within  $\pm 3$  per cent.

#### OTHER CONSIDERATIONS

A number of other factors must be taken into account before we can consider the practical use of thick aluminum targets and filters in a radiotherapy linear accelerator. (1) The target must not be an intense source of neutrons; aluminum is satisfactory from this point of view. (2) The target should not become intensely radioactive; again aluminum creates no difficulty since most of the activity is short lived. (3) The cooling of an aluminum target is not a consideration. (4) An argument could be made that a thick target of low  $Z$  material would give a larger effective source of x rays than a thick target of high  $Z$  material. This

could conceivably increase the size of the penumbra. Experiments designed to test this idea showed, however, that there was no difference. (5) The main problem involves space, since large thickness of target and filter is required and their replacement in a finished linac would require a complete redesign of the head. In a linac under design, however, these considerations should be taken into account.

#### CONCLUSIONS AND SUMMARY

The 25 MeV electron beam was extracted from a Varian Clinac-35 linear accelerator and made to produce x-rays in thick targets of different materials. The x-ray beams were flattened by filters of various materials.

We have found that an aluminum thick target gives a more penetrating beam in the forward direction than does a lead or tungsten target.

The x-ray yield in the forward direction from  $0-5^\circ$  is essentially the same for both aluminum and lead targets. At angles larger than  $10^\circ$ , a lead target shows a higher x-ray yield and a more penetrating beam than an aluminum target.

The flattening filter material is important. A more penetrating beam is produced if the flattening filter is made of aluminum rather than tungsten or lead.

With an aluminum target and an aluminum flattening filter, we obtain the same depth dose distribution from our linear accelerator as we do from our betatron unit operating at the same energy. In the betatron unit, the radiation is produced in a thin target of tungsten and filtered by aluminum.

For the situations that arise in radiotherapy we have shown that the beam from an aluminum target/aluminum flattening filter combination can be flattened just as easily as the beam from a lead target/lead flattening filter combination.

We conclude, therefore, that contrary

to conventional practice, low atomic number materials should be used for the targets and flattening filters of high energy radiotherapy linear accelerators.

We plan to extend our investigations of target and filter design to lower electron energies (10-20 MeV).

It is hoped that this paper will inspire manufacturers of new linacs to design the head to include aluminum targets and filters so that the optimum characteristics of the beam can be realized.

H. E. Johns, Ph.D.  
Physics Division  
The Ontario Cancer Institute  
500 Sherbourne Street  
Toronto, Ontario  
Canada M4X 1K9

The financial support of the Medical Research Council of Canada and the National Cancer Institute of Canada is gratefully acknowledged.

#### REFERENCES

1. BERGER, M. J., and SELTZER, S. M. Tables of Energy Losses and Ranges of Electrons and Positrons. Nuclear Science Series, Report Number 39, National Academy of Sciences, National Research Council, Publication 1133, Washington, 1964, pp. 205-268.
2. BERGER, M. J., and SELTZER, S. M. Bremsstrahlung and photoneutrons from thick tungsten and tantalum targets. *Phys. Rev.*, 1970, 2, 621-631.
3. HEITLER, W. The Quantum Theory of Radiation. Third edition. Oxford University Press, London, 1954.
4. JOHNS, H. E., RAWLINSON, J. A., and TAYLOR, W. B. Matrix dosimeter to study the uniformity of high energy x-ray beams. *AM. J. ROENTGENOL., RAD. THERAPY & NUCLEAR MED.*, 1974, 120, 192-201.
5. KOCH, H. W., and MOTZ, J. W. Bremsstrahlung cross-section formulae and related data. *Rev. Mod. Phys.*, 1959, 31, 920-955.
6. RAWLINSON, J. A., and JOHNS, H. E. Percentage depth dose for high energy x-ray beams in radiotherapy. *AM. J. ROENTGENOL., RAD. THERAPY & NUCLEAR MED.*, 1973, 118, 919-922.